Jour. Indian Association of Sedimentologists, Vol. 36, No. 1 & 2 (2019), pp.19-50
ISSN Online 2582 – 2020
ISSN Print 0970 – 3268

Depositional environment and Provenance of Pilikarar Formation, Central Narmada basin, Hoshangabad District, Madhya Pradesh, India

M. G. Kale[1*] and Ashwin S. Pundalik[2]
[1] Department of Geology, Savitribai Phule Pune University, Pune - 411 007, India.
Email: mgkale@unipune.ac.in
[2] Department of Geology, St. Xavier's College, Mumbai – 400 001, India.
Email: ashwin.pundalik@xaviers.edu

Abstract: The Pilikarar Formation comprised of coarser clastics, occur as isolated as well as coalescent cones and exhibit development of bouldery conglomerate lithofacies, with both clast supported and matrix supported varieties; representing debris flow and mud flow deposits of alluvial fan respectively. Caliche nodules and rhizoliths in the middle part of Pilikarar Formation indicate semiarid climatic conditions and related subaerial exposure. Immediacy of this alluvial fan to Son-Narmada-North fault indicates that this fault provided the basin depression, geomorphic contrast together with climate favoured the debris flow process to built alluvial fan.

Granulometric studies of these sediments reveal presence of wide range of size classes, polymodal nature, moderate to very poor sorting, positive skewness and leptokurtic to platykurtic distribution; supplementing fluvial environment of deposition. Thin section studies revealed quartzose arenitic nature, indicating mineralogical maturity of these sediments. The presence of ferruginous cement is suggestive of acidic and oxidising diagenetic conditions. Presence of illite, kaolinite and montmorillonite in these sediments, further supports derivation from soils developed on these rocks. Geochemical composition of these sediments supports mixed provenance and mineralogical maturity of these sediments. Paleotemperature derived from $\delta^{18}O$ content (-1.60 ‰) of calcrete indicate moderate temperature of 21.44°C for Pilikarar Formation, thereby indicating C3-C4 mixed vegetation with dominance of C3 vegetation. The low value of pCO_2 (154.6 ppmV) derived from $\delta^{13}C$ content (-9.25 ‰), and the $\delta^{18}O$ content (-1.60 ‰) suggests evaporation and evapotranspiration as the main process in calcite precipitation, indicating meteoric diagenesis related with semi-arid climatic conditions undergone by Pilikarar sediments. The mineralogical maturity is further supported by high ZTR index together with transparent heavy mineral assemblage of augite, epidote, staurolite, garnet, sillimanite, kyanite, sphene, hornblende, zoisite, monazite, anataze and low values of provenance sensitive indices; related to derivation of these sediments dominantly from Vindhyan Supergroup, with subordinate contribution from Deccan Trap Basalts and Mahakoshal Group.

INTRODUCTION

The Central Narmada basin of Peninsular India is one of the few regions of India where Quaternary deposits are very well developed and preserved. The Narmada River is the largest westerly

flowing river in to the Arabian Sea in India (Gupta et al., 2011), which flows through ENE-WSW trending Narmada-Son lineament. It is an ancient tectonic feature dated to be Precambrian (Choubey, 1971). This deep crustal structure of Narmada-Son lineament is inferred to have been initiated as a protocontinental suture during Late Archean-Early Proterozoic times and subsequently evolved as a rift generated cratonic margin during the Proterozoic times (Kale, 1986). The southern margin of central Narmada valley and northern margin of Purna-Tapti valley are defined by two almost east-west trending regional faults known as North Satpura and South Satpura faults respectively. Reactivation along these faults during Quaternary has given rise to accumulation of about 400 m thick Quaternary deposits in these valleys (Vaidyanathan and Ramakrishnan, 2008). Tiwari and Bhai (1997) recognized seven lithostratigraphic formations namely Pilikarar Formation, Dhansi Formation, Surajkund Formation, Baneta Formation, Hirdepur Formation, Bauras Formation and Ramnagar

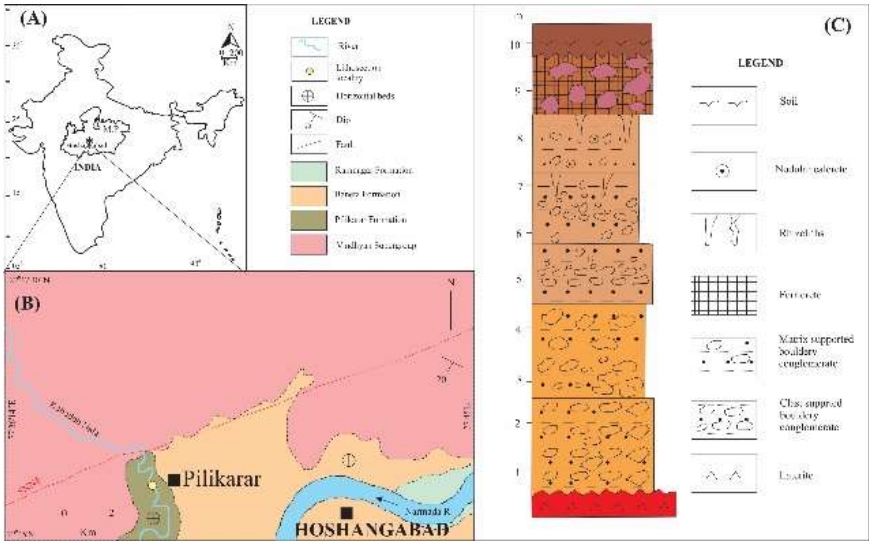

Figure 1:
A) Outline map of India showing location of study area.
B) Geological map of Pilikarar area, Central Narmada basin (modified after, Tiwari and Bhai, 1997), SNNF- Son Narmada North Fault (after, GSI, 1993; Mishra, 2015).
C) Lithosection of Pilikarar Formation, Central Narmada basin.

Formation in order of decreasing antiquity. On the basis of carried out field and laboratory studies, an attempt is made in this paper to reconstruct the sedimentation history of Pilikarar Formation.

STUDY AREA

Pilikarar Formation (Lower Pleistocene?) is the lowermost lithostratigraphic unit of Quaternary succession of Central Narmada basin. The Pilikarar Formation has unconformable contact with Baneta Formation (Early Upper Pleistocene) which is exposed to the east Pilikarar village and rest of the area is occupied by Proterozoic Vindhyan

Supergroup rocks (Fig. 1B). The Pilikarar Formation has very restricted areal extent and is exposed in Kaliadoh Nala; which is located 1 Km west of Pilikarar village (Fig. 1B). Here about 10 meter thick section of sediments belonging to Pilikarar Formation is well exposed.

METHODOLOGY

From the Pilikarar lithosection five samples namely PK-1A, PK-1, PK-2, PK-3, PK-4 and PK-5 were systematically collected, out of which two well cemented samples (PK-1A and PK-5) were selected for thin section preparation. These were studied under the optical microscope and modal analysis was carried out by using point counter. Four samples were subjected to granulometric studies by 'Sieve and pipette' method given by Ingram (1971) and Galehouse (1971) respectively, and heavy minerals were separated from fine sand fraction (2.0 Phi to 4.0 Phi) of these samples following method given by Carver (1971). Clays separated from four samples were analysed using Phillips X-ray diffractometer at Wadia Institute of Himalayan Geology, Dehradun. The geochemical studies of four samples representing matrix of conglomerate PK-1A, PK-1, PK-2 and PK-3) was carried out on XRF (Axios, PAN analytical) and ICP-MS (Thermo X series 2) at National institute of Oceanography, Goa. Accuracy and precision of the major oxide data is better than +4%, while accuracy of trace and rare earth elements was checked using USGS standards BIR-1 and DNC-1. LOI i.e. Loss on Ignition was determined at Wadia Institute of Himalayan Geology, Dehradun. For these samples, weathering indices such as CIA i.e. Chemical index of alteration ($(Al_2O_3/Al_2O_3+Na_2O+K_2O+CaO^*)$ X 100; Nesbitt and Young, 1982), PIA i.e. Plagioclase Index of Alteration ($[(Al_2O_3 – K_2O) / ((Al_2O_3 - K_2O) + CaO^* + Na_2O)]$ X 100; Fedo et al., 1995), CIW i.e. Chemical Index of Weathering ($[Al_2O_3 / (Al_2O_3 + CaO^* + N_{a2}O)]$ x 100; Harnois, 1988), a modified version of CIW i.e. CIW' for carbonate-bearing siliciclastic rocks ($[Al_2O_3/(Al_2O_3+Na_2O)]$ X 100; Cullers, 2000), ICV i.e. index of compositional variability ($(Fe_2O_3+ K_2O + Na_2O + CaO + MgO + MnO + TiO_2) / Al_2O_3$; Cox et al., 1995), WIP i.e. weathering index ($100 \times (CaO^*/0.72 + 2Na_2O/0.35 + 2K_2O/0.25 + MgO/0.9)$; Parker, 1970) and W index ($\exp.(0.203\ln(SiO_2) + 0.191\ln(TiO_2) + 0.296\ln(Al_2O_3) + 0.215\ln(Fe_2O_3) – 0.002\ln(MgO) – 0.448\ln(CaO^*) – 0.464\ln(Na_2O) + 0.008\ln(K_2O) –1.374$); Ohta and Arai, 2007) were calculated. Stable isotope composition of one rhizolith sample was determined at CSIR-National

Institute of Geophysical Research, Hyderabad, using Thermo Finnigan Delta plus XP Continuous Flow Isotope Ratio Mass Spectrometer (CF-IRMS) with attached preparation device Gas Bench II and robotic sampling arm (CG-PAL). Using the stable isotope values and following the procedure given by Friedman and O'Neil (1977), the temperature for calcite precipitation was calculated. Cerling (1999) has given method for calculating pCO_2 using $\delta^{13}C$ values following which, the value of pCO_2 for the rhizolith sample was estimated.

RESULTS

Field characteristics

The sediments of Pilkarar Formation rest unconformably over laterite with non-erosive contact, and on the top of these sediments, development of soil cover is noticed (Fig.1C). These sediments occur as small isolated (Fig.2A) as well as coalescent cones constituted of coarser clastic sediments with development of bouldery conglomerate lithofacies.

Bouldery conglomerate lithofacies is represented by thickly bedded, poorly sorted clasts ranging from granule to large boulders; floating in matrix consisting of sand, silt and clay. Their thicknesses vary from 1.5 to 2.5 m and these can be traced laterally up to 50 m. The clasts vary in size from 2 to 19.8 cm. The clasts of these conglomerates are angular to subangular with few subrounded clasts and at places slabby clast are also noticed. They are of sandstone, vein quartz, agate and laterite; floating in yellowish buff coloured matrix (Fig. 2B). Within this lithofacies two subfacies i.e. clast supported bouldery conglomerate and matrix supported bouldery conglomerate are present and are intermingling with each other (Fig. 2C). Within the clast supported bouldery conglomerate, concentration of boulders is observed in the middle as well as upper part (Fig. 2D). In the upper part of Pilikarar lithosection, clast supported bouldery conglomerate passes in to matrix supported bouldery conglomerate (Fig.1C and 2D). Decrease in the clast size is noticed in matrix supported bouldery conglomerate with dominance of pebble size clasts. Within this variety of conglomerate, development of nodular calcrete as well as rhizoliths are noticed (Fig.2D). Both normal as well as reverse grading of clasts from boulder to granule and from granule to boulder is noticed within this facies (Fig. 2B). In the uppermost part of this lithosection, the clasts are cemented by reddish brown ferruginous cement (Fig. 2E). Close up view of Fig. 2E shows angular to subrounded pebble to boulder

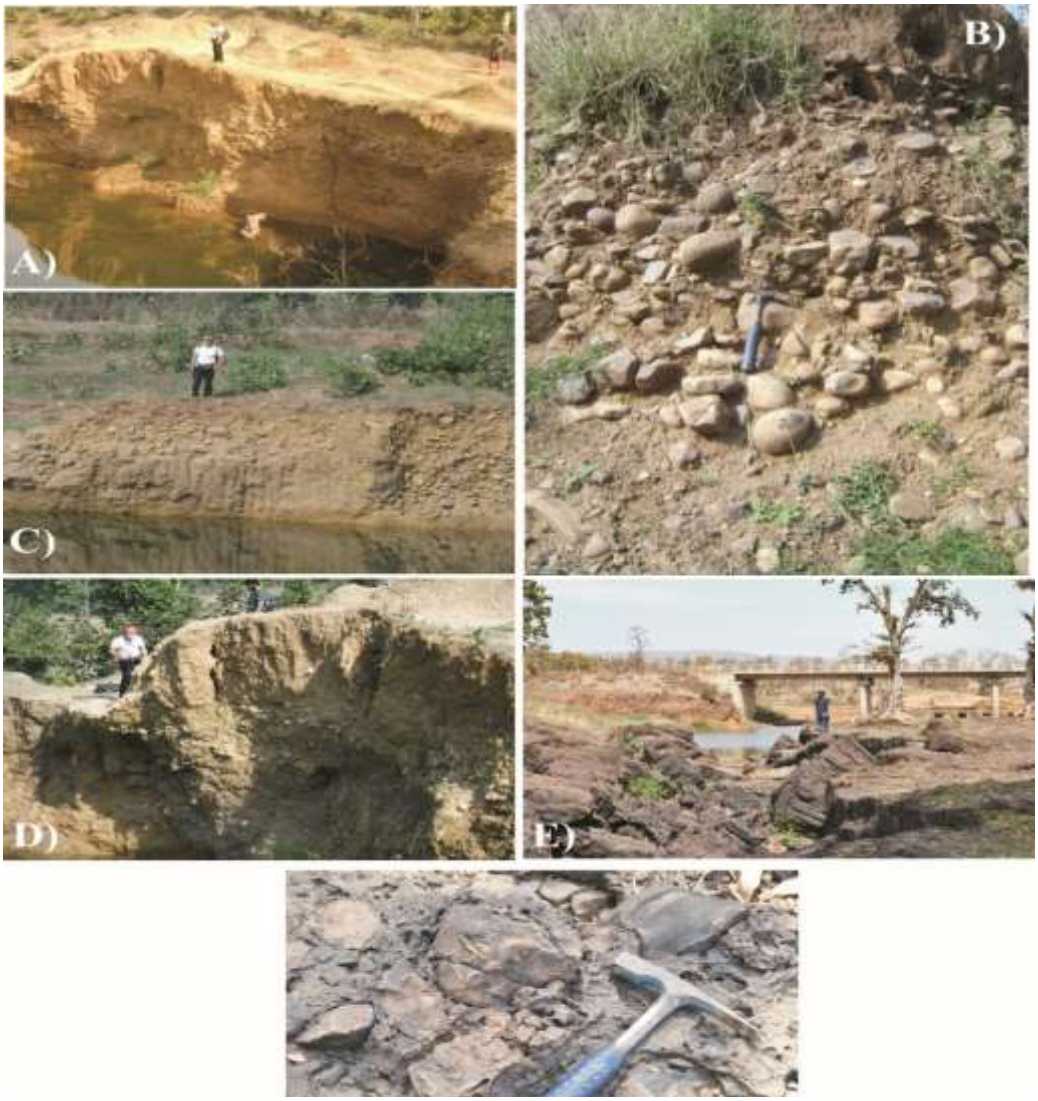

Figure 2:

A) Pilikarar Formation coarser clastics occuring as small isolated cone. Locality: Kaliadoh Nala, near Pilikarar.
B) Bouldery conglomerate consisting of subangular to rounded clasts of s andstone, basalt, vein quartz and laterite floating in yellowish buff coloured matrix consisting of sand, silt and clay. Note the normal as well as reverse grading of clasts.
C) Intermingling of clast supported bouldery conglomerate and matrix supported bouldery conglomerate.
D) Bouldery conglomerate exhibiting concentration of boulders in middle as well as upper part. Note vertical passage of clast supported bouldery conglomerate to matrix supported bouldery conglomerate. Development of nodular calcrete and rhizolith is noticed in the middle part.
E) Bouldery conglomerate in which clasts are cemented by reddish brown ferruginous cement.
F) Close-up view of 3e, exhibiting angular to subrounded pebble to boulder size clasts of sandstone bounded by reddish brown ferruginous cement.

clasts bounded by reddish brown ferruginous cement (Fig. 2F).

Thin section studies

In Pilikarar thin sections, framework grains show wide variation in grain size from silt to coarse sand, angular

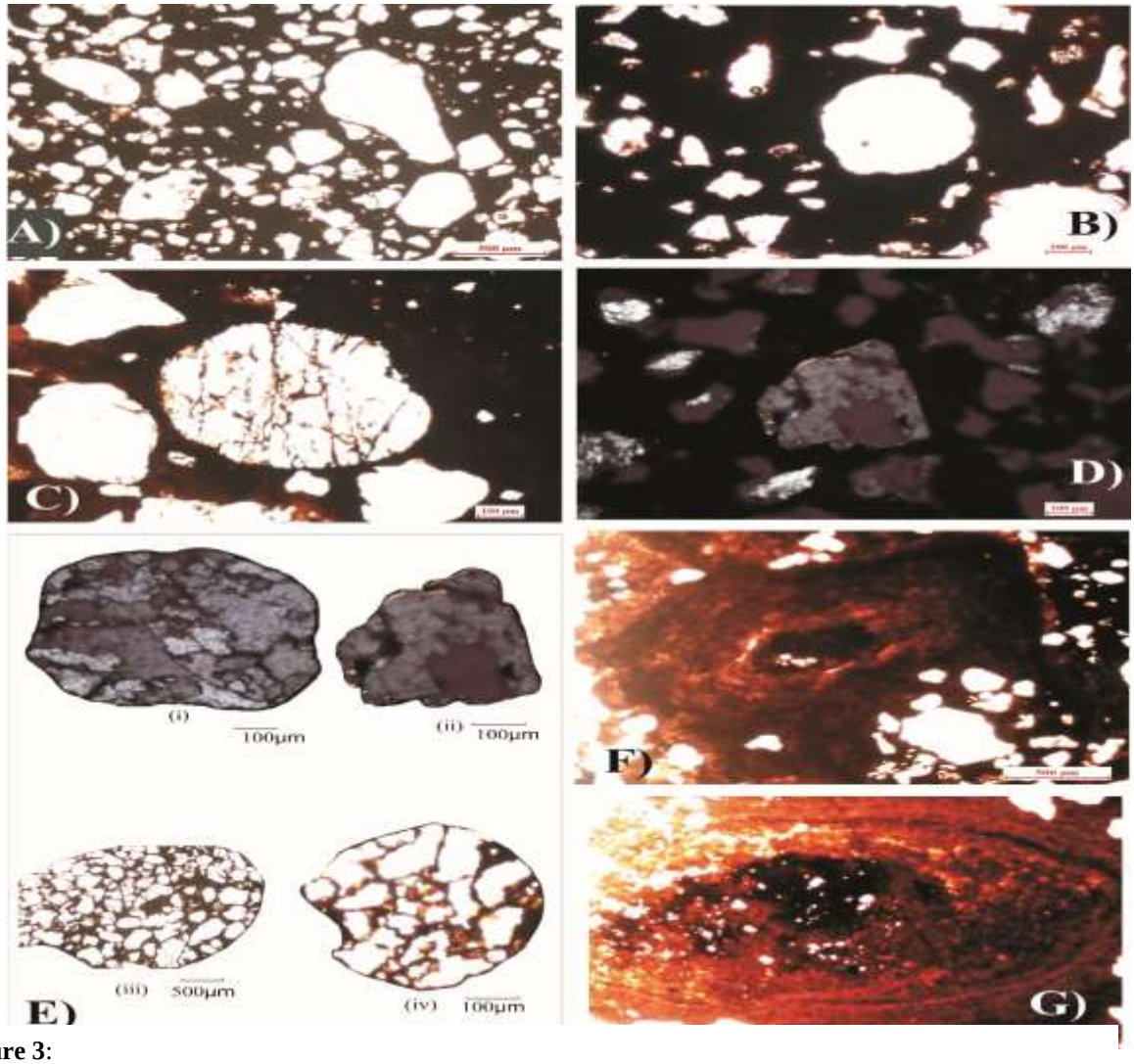

Figure 3:

A) Photomicrograph exhibiting extremely poorly sorted nature of framework grains floating in ferruginous cement (PPL).
B) Angular nature grains with occasional well rounded grain of quartz floating in ferruginous cement (PPL).
C) Embayment of dark brown ferruginous cement along the cracks of quartz grains (PPL).
D) Development of very thin isopachous rim of micritic calcite around the polycrystalline quartz grain (BCN).
E i) Polycrystalline quartz fragment consisting of large number of varying size constituent grains with sutured, irregular grain contacts (BCN).
E ii) Polycrystalline quartz fragment consisting of five varying size constituent grains with irregular grain contacts
E iii) Sandstone fragment consisting framework grains with wide variation in the size, bounded by ferruginous cement (PPL).
E iv) Subrounded medium grained sandstone fragment with fine to medium sand size framework grains floating in ferruginous cement (PPL).
F) Development of irregular concretions with in ferruginous cement (PPL).
G) Close up view of concretion with development of concentric lamination (PPL).

to subrounded nature and are observed to be floating in ferruginous cement (Fig. 3A). In these sediments, ferruginous cement is dominantly present (62.50% to 65.25%, av. 63.88%) and the framework constituents are dominated by quartz (31.23% to

33.07%, av. 34.27%) with negligible amount of K-feldspars (1.75% to 1.96%, av. 1.85%) and lithic fragments (2.03% to 3.20%, av. 2.62%); hence can be described as quartzose arenites (Okada, 1971) indicating mineralogically maturity. Within quartz, both monocrystalline and polycrystalline varieties are present. Within monocrystalline quartz, nonundulatory variety (17.09% to 18.33%, av. 17.71%) dominates undulatory variety (11.20% to 12.70%, av. 11.95%), which together dominates over polycrystalline quartz (1.44% to 3.54%, av. 2.49%). Majority of quartz grains are subangular in nature and occasionally well rounded grains of quartz are also noticed within these thin sections (Fig. 3B). Different varieties of polycrystalline quartz present include i) fragment consisting of large number of varying size constituent grains with sutured, irregular grain contacts (Fig. 3E, i and ii) consisting of five varying size constituent grains with irregular grain contacts (Fig. 3E, ii). Commonly within the quartz grains, presence of cracks is noticed, which are filled with dark brown ferruginous cement (Fig. 3C). Within K-feldspars, microcline predominates over orthoclase, and majority of feldspars are altered. Unstable lithic fragments present are dominantly of sandstones. The large sandstone fragment showing wide variation in the size of framework grains bounded by ferruginous cement is shown in Fig. 3E, iii; while Fig. 3E, iv exhibits subrounded medium grained sandstone fragment with fine to medium sand size framework grains floating in ferruginous cement. Occasionally development of very thin isopachous rim of micritic calcite around the framework grains (Fig. 3D) can also be seen in these thin sections. Within the ferruginous cement irregular concretions (Fig. 3F) and development of concentric lamination (Fig. 3G) is also noticed.

Granulometry

Granulometric studies of these sediments revealed presence of wide range of grain size classes ranging from -6.00 to 10.5 ϕ, polymodal grain size distribution, poor to very poor sorting (1.79 ϕ to 3.34 ϕ, av. 2.45 ϕ), positive skewness (0.27 ϕ to 1.26 ϕ, av. 0.66 ϕ) indicating their fine to coarse skewed nature and dominance of coarser admixture over finer and Platykurtic to very leptokurtic to (0.87 ϕ

Table 1: Heavy mineral frequency percentages along with provenance sensitive indices (Morton and Hollsworth, 1994, 1999 and Morton and Milne, 2012) and heavy mineral concentration indices (Garzanti and Ando, 2007) of sediments of Pilikarar Formation.

Sample No.	**PK-1**	**PK-2**	**PK-3**	**PK-4**	**Average**
Minerals					
Zr	63.63	51.93	46.48	46.29	**52.02**
To	5.05	22.45	8.72	9.07	**11.32**
Ru	4.04	1.45	1.36	0.98	**1.96**
Au	8.08	13.52	21.91	25.32	**17.21**
Ep	1.01	0.08	1.21	--	**0.58**
St	--	1.45	1.39	--	**0.71**
Gt	13.13	4.18	12.45	10.85	**10.15**
Sil	--	1.45	2.18	2.53	**1.54**
Ky	1.01	1.91	2.19	2.99	**2.03**
Sp	1.01	0.54	--	--	**0.39**
Zo	--	1.00	--	--	**0.25**
Mo	1.01	1.00	2.02	0.98	**1.25**
Hb	1.01	--	1.53	--	**0.64**
An	1.01	--	--	0.98	**0.50**
ZTR	72.72	75.83	56.56	56.34	**65.36**
PSI					
GZi	17.11	7.45	21.13	18.99	**16.17**
RZi	2.51	2.65	2.54	1.89	**2.40**
RuZi	5.97	2.72	2.84	2.07	**3.40**
Mzi	0.90	0.91	1.21	0.94	**0.99**
SZi	--	2.72	2.90	--	**1.41**
UTi	28.57	2.69	12.19	--	**10.86**
AmZRT	--	2.63	--	17.65	**5.07**
EpZRT	0.11	2.09	--	17.59	**4.95**
GtZRT	15.29	5.22	18.04	16.15	**13.68**
KyZRT	1.37	2.46	3.73	5.04	**2.52**

GZi	100X Garnet count/(Garnet + Zircon)
RZi	100 X TiO_2 mineral count / (TiO_2minerals+Zircon)
RuZi	100 X Rutile count / (Rutile+Zircon)
MZi	100 X Monazite count/ (Monazite + Zircon)
SZi	100 X Staurolite count / (Staurolite +Zircon)
UTi	100 X (Unstable total) / (Unstable + Tourmaline)
AmZRT	Amphibole / (Amphibole + Zircon + Tourmaline + Rutile)
EpZRT	Epidote / (Epidote + Zircon + Tourmaline + Rutile)
GtZRT	Garnet / (Garnet + Zircon + Tourmaline + Rutile)
KyZRT	Kyanite / (Kyanite + Zircon + Tourmaline + Rutile)

Zr- Zircon, To- Tourmaline, Ru-Rutile, Au- Augite, Ep- Epidote, St- Staurolite, Gt- Garnet, Sill- Sillimanite, Ky- Kyanite, Sp- Sphene, Zo- Zoisite, Spl- Spinel, Ch- Chlorite, Mo- Monazite, Hb- Hornblende, and An- Anatase, ZTR- Combined percentage of zircon, tourmaline and rutile, PSI- Provenance sensitive indices.

to 2.11 ϕ, av. 1.34 ϕ) related with mixing of two or more subequal populations. The gravel-sand-mud ratio for the clast supported conglomerate is 76:18:5, while for the matrix supported conglomerate it is 2:43:55. The log probability plots of these sediments exhibit development of better-sorted saltation population (slopes up to 78 ^{o}), poorly sorted suspension population (slopes up to 45 ^{o}) and better sorted surface creep population (slope up to 45^{o}).

Heavy mineral studies

The percentages of the transparent heavy minerals in the sediments of the Pilikarar Formation are presented in Table 1. Heavy mineral assemblage of Pilikarar Formation consists of 14 transparent heavy mineral species which include zircon, tourmaline, rutile, augite, epidote, staurolite, garnet, sillimanite, kyanite, sphene, zoisite, monazite, hornblende and anataze. Zircon (av.52.02 %) constitutes the half of the bulk transparent heavy mineral crop. The average ZTR index (Hubert, 1962) for these samples is 65.36. Most of the zircon and tourmaline grains are subrounded to rounded in nature with few euhehdral and subhedral grains (Fig.4.1 to 4.11). Many a times opaque inclusions are noticed within zircon grains (Fig. 4.4, 4.5, 4.6). Augite, epidote, staurolite, garnet, sphene and anataze grains are angular to subangular (Fig. 4.14 to 4.19). Rutile, sillimanite, kyanite, hornblende and zoisite occurs as elongated grains (Fig. 4.14, 4.15, 4.21, 4.22, 4.23, 4.25). For these sediments, various provenance sensitive indices of Morton and Hollsworth (1994, 1999) and Morton and Milne (2012) were calculated, and values of these indices are given in Table 2. The samples from Pilikarar Formation show low values of MZi (av.2.40), RZi (av.3.40), RuZi (av.0.99), SZi (av.1.41), UTi (av.10.86), AmZRT (av.1.00), EpZRT (av.0.89) and KyZRT (av.2.52) with slightly moderate values of GZi (av.16.17) and GtZRT (av.13.68) owing to high proportion of zircon in heavy mineral crop as well as high value of ZTR index.

Figure 4: Heavy mineral species from Pilikarar Formation.
1 to 6- Zircon, 7 to 11- Tourmaline, 12 and 13- Rutile, 14 and 15- Augite, 16- Epidote, 17- Staurolite, 18 and 19- Garnet, 20-Silimanite, 21- Kyanite, 22- Sphene, 23- Zoisite, 24- Monazite, 25- Hornblende and 26- Anatase.

X-ray diffraction studies

The X-ray diffraction studies of clays from Pilikarar Formation revealed illite (3.35 dA° –100 %) as dominant clay mineral with subordinate kaolinite(1.78 dA° – 7 % to 19 % and 1.53 dA° – 9 %) and montmorillonite (4.50 dA°-78 %, 2.50 dA° -36 %).

Geochemical studies

The obtained values of major oxides (weight percentages), trace element composition (ppm) and chondrite normalized rare earth element composition (ppm) of Pilikarar sediment samples are given in Table 2 and 3 respectively. Pilikarar sediments show high values of SiO_2/Al_2O_3 ratio as compared to Na_2O/K_2O ratio and Fe_2O_3/K_2O ratio, due to their high quartz content compared to feldspars and ferromagnesian minerals (Pettijohn et al., 1972; Herron, 1988). On major oxide provenance discrimination diagrams of Roser and Korsch (1988), samples from

Sample No.	**PK-1A**	**PK-1**	**PK-2**	**PK-3**	**Average**
Oxides					
SiO_2	43.42	64.66	68.82	78.72	**63.91**
Al_2O_3	8.13	9.86	6.96	7.55	**8.13**
TiO_2	1.01	0.73	0.58	0.70	**0.76**
Fe_2O_3	38.71	14.66	3.94	4.41	**15.43**
MnO	0.19	0.17	0.03	0.10	**0.12**
MgO	0.14	0.76	0.94	0.75	**0.65**
CaO	0.16	0.40	6.87	0.87	**2.08**
Na_2O	0.10	0.17	0.22	0.64	**0.28**
K_2O	0.22	1.67	1.06	0.73	**0.92**
P_2O_5	0.15	0.06	0.03	0.02	**0.07**
LOI	7.76	6.86	10.55	5.50	**7.67**
Total	**100**	**100**	**100**	**100**	100
Weathering indices					
CIA	93.65	80.66	78.78	72.25	**81.34**
PIA	96.15	93.49	88.93	76.24	**88.70**
CIW	96.26	94.61	90.58	78.19	**89.91**
CIW '	98.09	97.23	95.06	87.76	**94.54**
ICV	3.34	1.50	1.08	1.15	**1.77**
WIP	8.17	16.16	13.63	16.49	**13.61**
W index	98.68	95.45	59.93	74.09	**82.04**

Table 2: Major element composition (Wt %) and weathering indices of sediments of Pilikarar Formation.

Pilikarar Formation show mixed provenance i.e. quartzose sedimentary and mafic igneous (Fig. 5). On A-CN-K ternary diagram of Nesbitt and Young (1984,1989) Piliarar samples plot near illite and kaolinite field (Fig.6A). The PIA values of the sediments plotted on CaO*-(Al_2O_3+K_2O)-Na_2O diagram (Fig.6B) plot near Al_2O_3 + K_2O apex, indicating intense weathering of plagioclase felspar (Fedo et al.,1995; Purevjav and Roser, 2013). The intensity and duration of weathering of these sediments are further evaluated by examining the relationships among alkali and alkaline earth elements (Nesbitt and Young, 1982) using weathering indices discussed above. CIA and CIW are used to evaluate weathering of sediment source (Nesbitt and Young, 1982; Harnois, 1988), PIA evaluates degree of plagioclase alteration (Fedo et al., 1995), CIW' is used as measure of source weathering for carbonate bearing siliciclastic rocks (Cullers, 2000), ICV is used to evaluate mineralogical maturity (Cox et al. 1995) and WIP and W index to determine the degree of recycling (Parker, 1970; Ohta and Arai, 2007). These weathering indices in combination are used to evaluate weathering of source, nature of source as well as mobility of elements during diagenesis and leaching (Jafarzadeh and Hosseini-Barzi, 2008). The values of these

weathering indices for sediments of Pilikarar Formation are given in Table 2. On the plot of WIP versus CIA (Garzanti et al., 2013b), Pilikarar sediments show low WIP values associated with high CIA values and fall within the field of recycled sediments (Fig 6 C). W index of the sediments under study varies from 59.93 to 98.68% (Table 2), thereby indicating moderate to high intensity of weathering.

For discriminating tectonic setup of sediment deposition, Verma and Armstrong-Altrin (2013) have proposed a new discriminant-function-based multi-dimensional diagram, in which Pilikarar sediments plot within the continental rift field (Fig.7A). On the geochemical discrimination diagrams of siliciclastic sediments (Verma and Armstrong-Altrin, 2016), samples from Pilikarar Formation plot in passive margin field (Fig. 7B and 7C).

Pilikarar sediments show enrichment in transition trace elements and LILE's except Rb and U (Table 3, Fig. 8A). In Pilikarar Formation, concentration of transition trace elements, LILE's and HFSE's decreases from clast supported conglomerate to matrix supported conglomerate (Table 3). On the Th/Sc versus Zr/Sc binary diagram (Fig. 9) of McLennan et al.(1993), samples from Pilikarar Formation show higher value of Zr/Sc and narrow range of Th/Sc. The chondrite normalized (Lodders and Fegley, 1998) rare earth element composition of Pilikarar sediments is given Table 3 and the prepared plots are exhibited in Fig. 8B. These sediments exhibit enriched LREE and depleted HREE, and negative europium anomaly (Fig. 8B) and negative Ce anomaly (Except for PK-1A). They show fractionated REE pattern characterized by high values (av. 10.82) of La/Yb ratio (Xie et al., 2017). La/Sm value ranging from 3.04 to 4.30 for the Pilikarar sediments suggests enrichment of LREE while low value of Gd/Yb ratio is reflected in flat HREE pattern (Banerjee and Banerjee, 2010). The ratios of $(La/Lu)_n$, Co/Th, La/Sc, Cr/Th, and Th/Sc were also determined which are sensitive to the nature of the source of the sediments (Tao et al., 2014; Tawfik et al., 2017) and are given in Table 4.

Sample No.	**PK- 1A**	**PK- 1**	**PK- 2**	**PK- 3**	**Average**
Element					
Li	0.67	1.04	0.83	1.02	**0.89**
Be	7.25	6.07	3.34	3.57	**5.05**
Sc	1.54	0.94	0.59	0.68	**0.94**
V	5.03	2.57	0.72	0.94	**2.32**
Cr	1.25	1.08	0.45	0.52	**0.82**
Co	1.98	1.87	0.65	1.18	**1.42**
Ni	0.97	0.90	0.57	0.68	**0.78**
Cu	5.74	2.69	0.95	1.14	**2.63**
Zn	0.40	0.42	0.48	0.39	**0.42**
Ga	1.88	2.15	1.33	1.29	**1.66**
Rb	0.19	1.37	0.85	0.83	**0.81**
Sr	0.13	0.14	0.29	0.22	**0.20**
Y	0.80	1.44	0.75	0.73	**0.93**
Zr	0.80	0.83	0.66	0.63	**0.73**
Nb	1.30	1.59	1.10	1.31	**1.33**
Sn	0.55	0.97	0.60	0.82	**0.74**
Sb	5.30	3.21	1.33	1.49	**2.83**
Cs	0.30	1.86	1.30	1.29	**1.19**
Ba	0.80	0.99	0.68	0.55	**0.76**
Th	0.60	1.23	0.88	0.90	**0.90**
U	1.63	1.12	0.76	1.06	**1.14**
Pb	0.30	0.21	0.10	0.13	**0.19**
La	103.36	176.00	108.60	120.38	**127.09**
Ce	241.29	201.77	115.48	142.0	**175.14**
Pr	78.44	107.23	66.69	76.88	**82.31**
Nd	92.70	96.91	56.20	66.87	**78.17**
Sm	33.99	42.88	25.25	28.39	**32.62**
Eu	21.16	25.37	14.49	15.56	**19.14**
Gd	26.75	32.59	19.13	21.01	**24.87**
Tb	19.97	25.00	14.24	15.24	**18.61**
Dy	15.21	19.29	11.04	11.48	**14.25**
Ho	12.80	17.13	9.66	9.73	**12.33**
Er	12.99	17.80	10.16	9.91	**12.71**

Tm	12.68	17.44	10.16	9.72	**12.5**
Yb	12.28	16.16	9.84	9.30	**11.89**
Lu	11.48	15.92	9.64	9.04	**11.52**
Σ REE	**695.09**	**811.50**	**480.58**	**545.52**	**633.17**
La/Lu	9.00	11.06	11.27	13.32	**11.16**
Eu/Sm	0.62	0.59	0.57	0.55	**0.58**
Eu/Eu*	0.70	0.68	0.66	0.64	**0.67**
La/Yb	8.42	10.89	11.04	12.94	**10.82**
Gd/Yb	2.18	2.02	1.94	2.26	**2.10**
La/Sm	3.04	4.10	4.30	4.24	**3.92**
Y/Ho	1.31	1.77	1.63	1.57	**1.57**

1: Rudnick and Gao (2003),

2: Lodders and Fegley (1998).

Table 3: UCC normalized[1]Trace element (ppm) and chondrite[2] normalized rare earth element (ppm) composition of sediments of Pilikarar Formation.

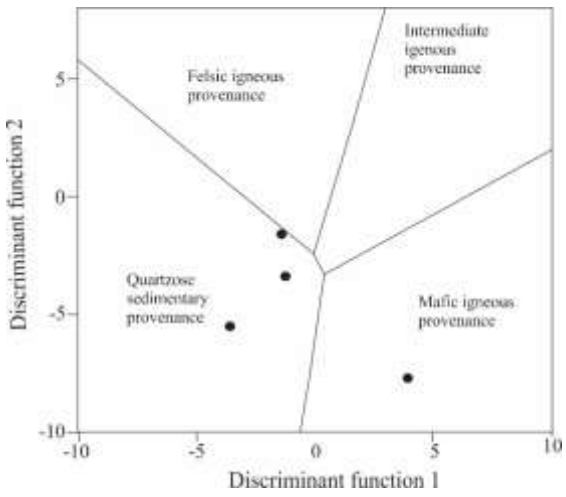

Figure 5: Discriminant function diagram for the provenance signatures of sediments from Pilikarar Formation using raw oxides (after Roser and Korsch, 1988).

Discriminant function 1= -1.773TiO2 + 0.607Al2O3 + 0.76Fe2O3 (total) - 1.5MgO + 0.616CaO + 0.509Na2O -1.224K2O - 9.09

Discriminant function 2= 0.445TiO2 + 0.07Al2O3 - 0.25Fe2O3 (total) - 1.142MgO + 0.438CaO + 1.475Na2O + 1.426K2O-6.861

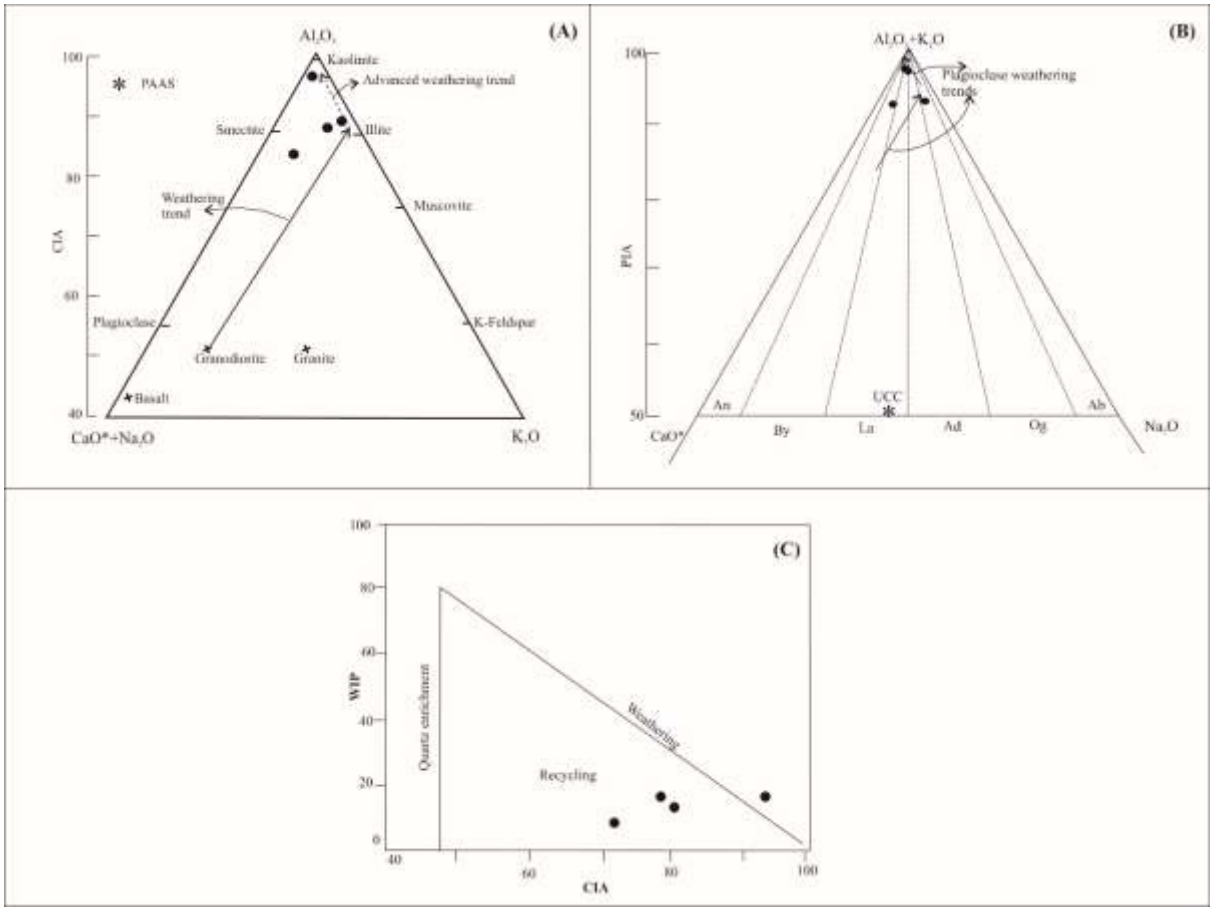

Figure 6:

A) (Na_2O+CaO)-Al_2O_3-K_2o diagram showing the weathering trends (modified after Nesbitt and Young 1984, 1989; data for granite, basalt and granodiorite after Le Maitre, 1976; Purevjav and Roser, 2013).

B) CaO*-(Al_2O_3+K_2O)-Na_2O diagram showing the weathering trends (modified after Nesbitt and Young 1982, Positions of plagiclase feldspars after Purevjav and Roser, 2013). An, By, La, Ad, Og, Ab – anorthite, bytownite, labradorite, andesine, oligoclase, and albite, respectively.

C) WIP versus CIA plot for sediments of Pilikarar Formation (after Garzanti et al., 2013b).

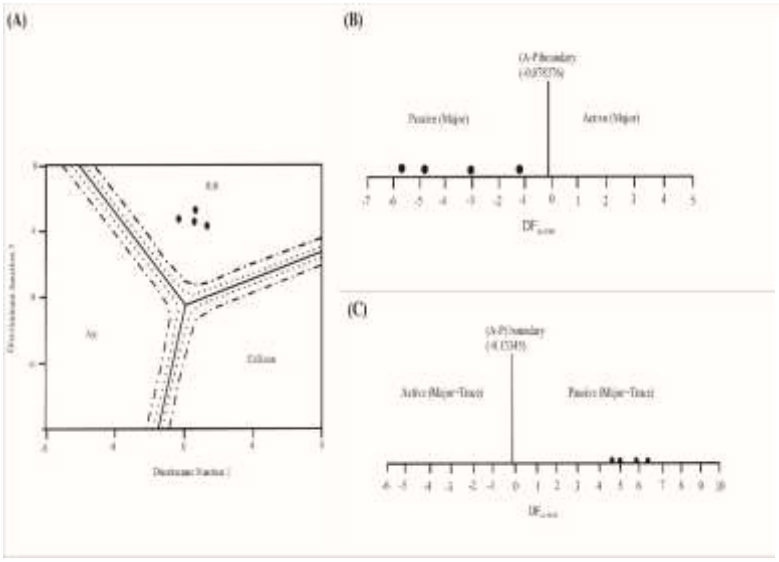

Figure 7:

A) Discriminant function multidimensional diagrams for sediments of Pilikarar Formation, the probability boundaries for 70% and 90% probabilities are also shown as dotted and dashed curves respectively.

B) Major element based multidimensional discriminant function diagram of sediments of Pilikarar Formation.

C) Major and trace element based multidimensional discriminant function diagram of sediments of Pilikarar Formation (after Verma and Armstrong-Altrin, 2016).

Jour. Indian Association of Sedimentologists, Vol. 36, No. 1 & 2 (2019), pp.19-50
ISSN Online 2582 – 2020
ISSN Print 0970 – 3268

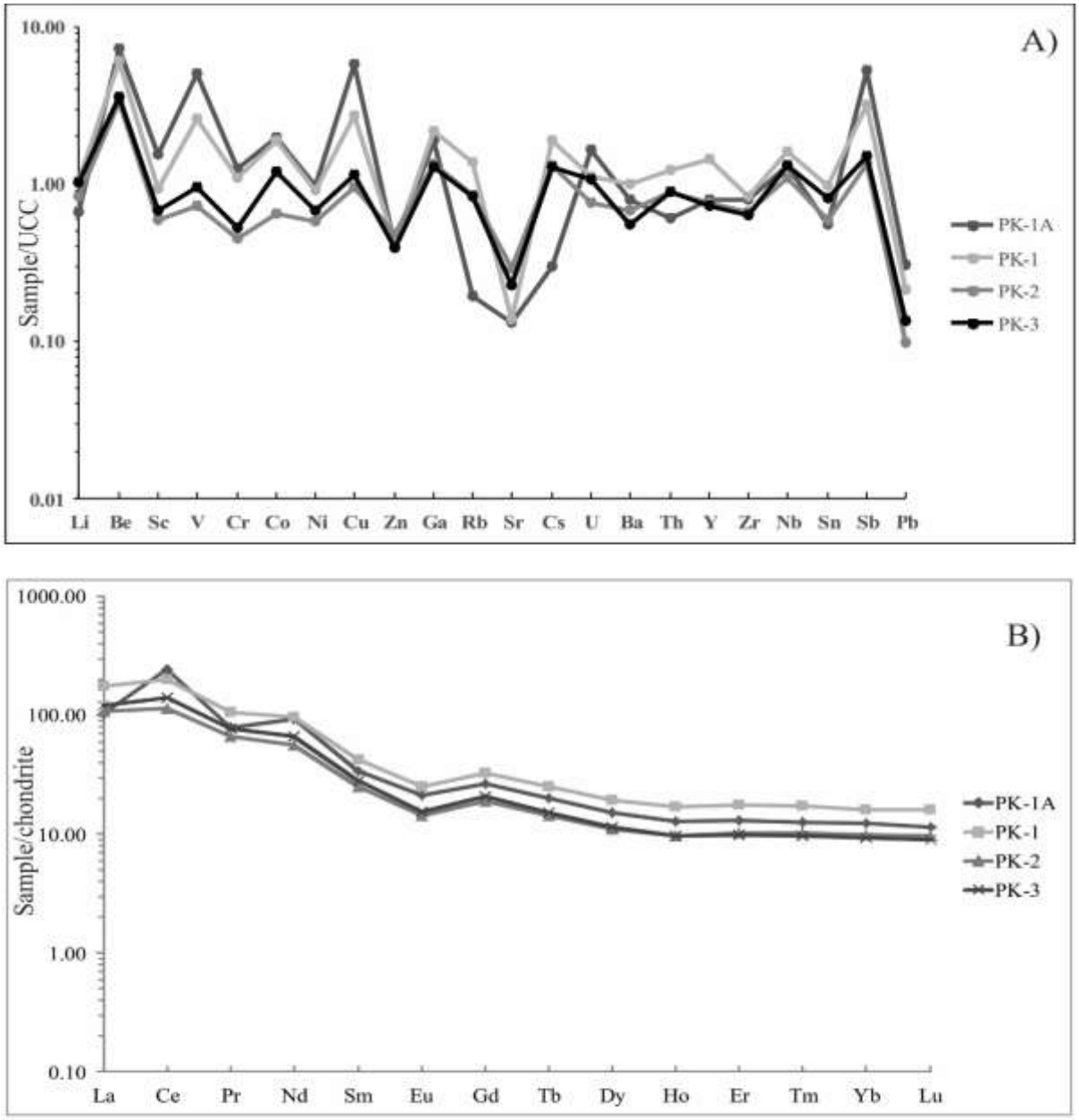

FIG. 8: A) UCC normalised trace element distribution pattern in sediments of Pilikarar Formation. B) Chondrite normalised rare earth element pattern in sediments of Pilikarar Formation.

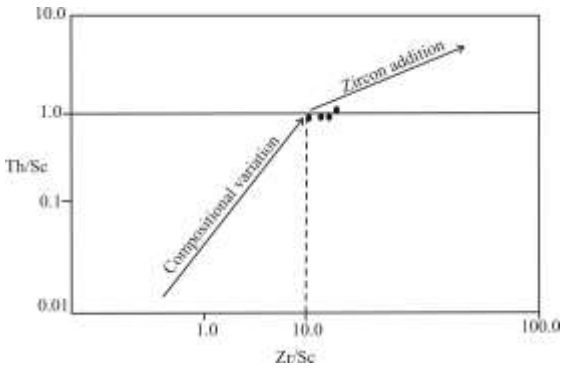

Figure 9: Th/Sc versus Zr/Sc plot for sediments of Pilikarar Formation (after McLennan etal., 1993).

	Pilikarar Sediments Range	**Average**	Sandstones[1]	Sediments from felsic source[2]	Sediments from mafic source[3]	UCC[4]	PAAS[5]
Eu/Eu*	0.64-0.70	0.67	0.71-0.95	0.40-0.94	0.71-0.95	0.66	0.71
$(La/Lu)_n$	9.0-13.32	11.16	4.37-8.27	3.0-27.0	1.10-7.0	10.39	9.86
Th/Sc	0.29-1.11	0.80	0.17-0.59	0.84-20.5	0.05-0.22	0.75	0.91
Cr/Th	4.45-18.11	8.53	21.69-67.93	4.0-15.0	25-500	8.76	7.53
Th/Co	0.19-0.82	0.46	0.17-0.43	0.67-19.4	0.04-1.40	0.61	0.63

1, 2 and 3: Cullers (1988, 1994, 2000), Cullers and Podkovyrov (2000).

4: Rudnick and Gao (2003).

5: Taylor and McLennan (1985).

Table 4: Range of elemental ratios of sediments of Pilikarar Formation compared to the ratios in similar fractions derived from felsic rocks, mafic rocks, upper continental crust and PAAS (After Tao et al., 2014).

Stable isotope studies

The obtained values of stable isotopes of oxygen and carbon for the rhizolith sample are negative i.e. the $\delta^{13}C$ content is -9.25 ‰ and $\delta^{18}O$ content is -1.60‰. According to Hays and Grossman (1991), $\delta^{18}O$ of meteoric calcite cement is an indicator of paleotemperature. The rhizolith from Pilikarar Formation is characterized by moderate paleotemperature value of 21.44ºC. The $\delta^{13}C$ of soil carbonates has been used as a proxy for estimating paleoatmospheric pCO_2 (Cerling, 1999;Ekart et al. 1999; Robinson et al., 2002). The calculated value of $pCO_2$for rhizolith of Pilikarar Formation is 154.6 ppmV.

DISCUSSION

The Pilikarar Formation resting unconformably on laterite, is characterized by development of bouldery conglomerate facies representing debris flow deposits of alluvial fan (Reineck and Singh, 1980; Blair and McPherson, 1994, 2009; Chamyal et al., 1997; Sohn et al., 1999; Reading, 2006; Miall, 2006; Collinson et al., 2006; Franke et al., 2015; Chen et al., 2017). Alluvial fans are a form of fluvial depositional system characterized on the basis of geomorphic

character rather than by a characteristic fluvial style (Miall, 2006). They represent the sedimentary record of upslope fluvial processes, controlled by the interaction between tectonics and climate, infused with the complex signatures of internal autogenic processes (Brooke et al., 2017). Alluvial fans are aggradational sedimentary deposits shaped overall like a segment of a cone radiating down slope from a point where a channel emerges from mountainous catchment (Bull, 1977; Blair and McPherson, 2009). The semi-conical shape of the fans is formed due to episodic avulsions of the active channel from a fixed fan apex (De Haas et al., 2018).The Pilikarar sediments under study represent debris flow dominated fan of Stainstreet and McCarthy (1993).

Debris flows are slurry-like flows of varied grain size, concentration, velocity, internal dynamics and therefore represent the most significant type of sediment gravity flow with respect to the volume of sediment delivered to the alluvial fans, which have been studied extensively (Johnson, 1970; Renwick, 1977). They are water-laden masses of sediment with volumetric sediment concentrations generally exceeding 40% (Costa, 1988; Iverson, 1997; De Haas et al., 2018). They represent extreme form of hyperconcentrated flow in which silt to boulder size grains are set in a matrix of clay grade fines and water, possess high flow density due to high concentration of suspended sediment which increases the buoyancy effect that mobilizes larger clasts (Jakob and Hungr, 2005;Ghinassi and Ielpi, 2016). In semi-arid settings like in the area under study, debris flows are generated by rare but intense rainstorm and such large energy outburst floods flush accumulated debris from the catchment valley (Reading, 2006). The resultant deposits commonly are disorganized, massive, poorly sorted, contain matrix and are clast supported, matrix supported or both, depending on position in the deposit as observed in the present case (Blair and McPherson, 1994; Chen et al., 2017). The Pilikarar alluvial fan lies at the base of Vindhyan range and is in close proximity of Son-Narmada North Fault (GSI, 1993; Mishra, 2015), therefore it is inferred that Son Narmada North Fault provided the basin depression, accommodation space and geomorphic contrast; though climate also a contributed in the debris flow process that constructed the Pilikarar alluvial fan (Chamyal et al., 1997; Chen et al., 2017). The development of isolated caliche nodules and rhizoliths is considered to be representative of secondary processes operating during inactive period between fan aggradations and semiarid climatic conditions prevailing

during the deposition of these sediments related with subaerial exposure of these sediments (Allen, 1974; Reading, 1981; Blair and McPherson, 1993). The granulometric studies of these sediments reveal the presence of wide range of size classes, polymodal grain size distribution, moderately sorted to very poorly sorted nature, dominance of positive skewness and leptokurtic nature and the shape of log probability plots of these show similarity to the plots of fluvial sediments thereby supporting fluvial deposition of sediments of Pilikarar Formation (Visher, 1969; Reineck and Singh, 1980; Reading, 1981). The quartzose arenitic nature of Pilikarar sediments indicates mineralogical maturity (Okada,1971). Presence of polycrystalline quartz grains that consists of varying size constituent grains with sutured, irregular grain contactsis suggestive of gneissic derivation and their rounded nature, together with occasional presence of well-rounded quartz in these sediments indicates its polycyclic nature (Young, 1976; Blatt, 1992). The presence sandstone fragments in these sediments suggests their derivation from the sandstones of Vindhyan Supergroup exposed to the north of Pilikarar. The isopachous rim of micritic calcite around the framework grain is suggestive of meteoric vadose diagenesis initially undergone by these sediments (Longman, 1980; Tandon and Friend, 1989; Tucker and Wright, 1990; Morse and Mackenzie, 1990). The presence of ferruginous cement in large volume particularly in upper part of Pilikarar section, is the result of diagenesis of these sediments under then prevailing oxidizing and acidic conditions (Tucker, 2001; Kettanah et al., 2014). Presence of ferruginous cement along the cracks of framework grains is the product of displacive cementation (Braithwaite, 1989). Heavy mineral suite of Pilikarar Formation is characterized by dominance of zircon (av. 51.56 %) and have moderately high ZTR index of 65.36with subrounded to rounded nature of zircon, tourmaline and rutile grains support mineralogical maturity of the sediments and suggest polycyclic nature derived from Vindhyan Supergroup sediments exposed to the north and northeast of Pilikarar. The observed yellowish brown tourmaline is considered by Blatt et al. (1972), to be representative of metamorphic source. The presence of wine red rutile in these sediments is indicative of high grade metamorphic provenance (Force, 1980). The derivation of these sediments from Precambrian granites and metamorphic provenance is further supported by presence of staurolite, garnet, sillimanite, kyanite, sphene, zoisite, spinel, chlorite, hornblende, anataze. The

appreciable amount of augite in this assemblage further suggests that during Pilikarar sedimentation along with Precambrian granites, metamorphics and Vindhyan Supergroup sediments, Deccan Trap basalts were also present in the source area. The samples belonging to Pilikarar Formation are characterized by very low values (<6.00) of all the provenance sensitive indices (RZi, RuZi, MZi, SZi, UTi, AmZRT, EpZRT, and KyZRT) except GZi (av. 16.17) and GtZRT (av. 13.68) which is related to low to moderate garnet, TiO_2 bearing minerals, rutile, unstable minerals and very low monazite, staurolite content. The X-ray diffraction studies of clays of these sediments support the petrographic and heavy mineral analysis of these sediments. Following Weaver (1989), the presence of illite and kaolinite are considered to be derived from Precambrian metapelites, shales, and the montmorillonite is derived from the soils developed on Deccan Trap basalts. The presence of illite in the Pilikarar sediments is considered to be derived from rocks of Vindhyan Supergroup exposed to the north of Pilikarar (Soni et al., 1987; Mohammadi et al., 2014).

Major oxide geochemistry of sedimentary rocks can be one of the determining factors for sediment maturity, provenance, weathering and tectonic setting of deposition. High values of SiO_2/Al_2O_3 ratio which is sensitive to sediment recycling and weathering process (Roser and Korsch, 1986; Roseret al., 1996; Liu et al., 2007)and the low values of Fe_2O_3/K_2O (Herron, 1988), suggest chemical maturity of Pilikarar sediments owing to their quartzose arenitic nature. Based on discriminant functions of Roser and Korsch (1988), Pilikarar Formation shows evidences of derivation from mixed provenance namely mafic igneous (Deccan basalt) and Quartzose sedimentary (Vindhyan Supergroup), thereby supporting petrography and heavy mineral studies. CIA values of sediments of Pilikarar Formation (av. 81.34%) together with CIW' (av.94.54%), ICV (av.1.77) and WIP (av.13.61) are suggestive of varied provenance, recycled nature of these sediments and indicate intense weathering of the source (Parker, 1970; Nesbitt and Young, 1982; Cox et al., 1995;Fedo et al., 1995; Bahlburg and Dobrzinski, 2009; Xie et al. 2017). With quartz enrichment, the value of WIP decreases, while CIA value remains unaffected(Xie et al., 2017). The plot of Garzanti et al. (2013b) thus distinguishes between first-cycle and recycled sediments (Garzanti et al., 2013a, 2013b; Xie et al., 2017), where recycled sediments plot in the field between the quartz enrichment trend and the UCC

weathering trend closer to the X-axis (Xie et al., 2017). The position of Pilikarar sediments on this plot (Fig. 6C) supports their recycled, quartzose arenitic nature and derivation mainly from Vindhyan Supergroup rocks as observed in petrographic, heavy mineral studies. High values of PIA (av. 88.70%) indicate intense weathering of feldspars (Purevjav and Roser, 2013) supporting presence of highly altered feldspars in thin sections. The high values of W index of Ohta and Arai (2007) also justify the absence of plagioclase feldspars in the thin sections. As observed in the diagrams of Verma and Armstrong-Altrin (2013) and Verma and Armstrong-Altrin (2016), the samples from Pilikarar Formation plot within the passive margin continental rift field, which is well in agreement with intracratonic rift setting of the Narmada basin (Ghosh, 1976; Verma and Banerjee, 1992).

The trace elements such as Th, Sc, Cr and Co are extensively used to reconstruct the sediment provenance (Armstrong-Altrin et al., 2017). Thorium (9.48 ppm) and Ba (av.474.23 ppm) content of Pilikarar sediments is slightly less than that of UCC (10.5ppm and 628ppm; Rudnick and Gao, 2003). According to McLennan and Taylor (1991), concentration of Zr, Hf and Ti in sediments is greatly affected by hydraulic sorting and heavy mineral fractionation, hence the enrichment of Zr (av. 140.68 ppm) in these sediments under study seems to be directly proportional to abundance of zircon (av. 52.02 %) in these sediments. Th/Sc ratios higher than 0.8, along with the higher values of Zr/Sc (11.87) in these sediments, are indicative of an input from mature and/or recycled sources, zircon accumulation by sediment recycling and sorting (Ali et al., 2014;McLennan et al., 1993; Armstrong-Altrin et al., 2013) and can be related to the derivation of Pilikarar sediments from the matured sediments. Narrow range of Th/Sc in the samples of Pilikarar Formation indicates their derivation from mature and/or recycled source (Ali et al., 2014) i.e. mainly from Vindhyan Supergroup rocks, which substantiates clast composition as well as thin section results. Th/U and Th/Sc ratios of the sediments under study (av. 3.38 and 0.80 respectively) roughly match with UCC value of 3.8 and 0.75 (McLennan and Taylor, 1991; Liu et al., 2007; Rudnick and Gao, 2003). Elemental ratios such as Th/Sc, Th/Co and Cr/Th are extremely useful in determining provenance of the sediments (Tao et al., 2014; Tawfik et al., 2017). Comparison of these ratios with the sediments derived from felsic and mafic rocks, and UCC further supports the mixed provenance of Pilikarar sediments (Table

6). The depletion in Rb and its poor correlation with Al_2O_3 (r = -0.12) is attributed to deficiency of feldspars and/or intense chemical weathering and recycling (Tawfik et al., 2017), hence supporting the less proportion of feldspars and alteration of feldspars observed in thin section studies. Slightly depleted U in these sediments indicates weathering and recycling which results in oxidation of insoluble U^{4+} to soluble U^{6+}, and loss of U due to solution (McLennan and Taylor, 1991; Liu et al., 2007). Sr content of av. 63.09 ppm of these sediments is indicative of meteoric diagenesis of these sediments as meteoric water contains up to 150 ppm of Sr (Flugel, 1982). However, considerable depletion of Sr compared to UCC (320 ppm) can be attributed to loss of Sr during intense weathering (Kamber et al., 2005) which is in well accordance with the weathering indices.

REE patterns of the sediments are interpreted to reflect the average continental crust and thus negative Eu anomaly found in sedimentary rocks is similarly interpreted to be a feature of upper continental crust (McLennan, 1989).Thus, the obtained rare earth element composition of Pilikarar sediments showing enrichment in LREE and depletion in HREE, with negative Eu and Ce anomalies reflects the composition of upper continental crust (McLennan, 1989). Negative Ce anomaly characteristic of tholeiitic basalt(Henderson ,1984), hence its presence in Pilikarar sediments suggests derivation from Deccan Trap basalts, which is supported by presence of appreciable amount of augite in heavy mineral assemblage of these sediments. REE's are insoluble and present in very low concentrations of river and sea water; hence, the REE present in sediments are chiefly transported as particulate matter and reflect chemistry of their source (Rollinson, 1993). The Eu/Sm ratio (av. 0.58) of these sediments is close to the upper limit of the range (Eu/Sm 0.16 to 0.55) for average basalt (Henderson, 1984) and significantly lower than that of UCC (0.21). The Y/Ho ratio for these sediments (av. 1.57) is also close to that of UCC (1.47) (Piper and Bau, 2013). Thus major, trace and rare earth element compositions of Pilikarar sediments are suggestive of derivation from Vindhyan Supergroup sediments, Deccan Trap basalts and dykes from Narmada Valley (Roser and Korsch, 1988; Mahoney, 1988; Seth et al., 2009).

The obtained value -9.25 ‰ of $\delta^{13}C$, and -1.60 ‰ of $\delta^{18}O$ of the rhizolith in the Pilikarar Formation lie well within the range of world calcrete between -12 to + 4 for $\delta^{13}C$ and -9 to +3 for $\delta^{18}O$; as given by Talma and Netterberg (1983) and Salomans and Mook, (1986 a, b). The observed $\delta^{18}O$

value of -1.60 ‰ is suggestive of input of meteoric water and related meteoric diagenesis, as $\delta^{18}O$ of pedogenic carbonate is considered to be in equilibrium with that of soil water, while isotopic composition of soil water is related to that of meteoric water(Srivastava, 2001; Khadkikar et al., 2000). The obtained isotopic compositions of calcretes support pedogenic and /or shallow groundwater origin for the calcretes under study (Cerling, 1984; Beckner and Mozley, 1998; Brlek and Glumec, 2014). The negative stable isotopic composition of rhizolith ($\delta^{18}O$ = -1.60 ‰ and $\delta^{13}C$ = -9.25 ‰) are suggestive of vadose diagenetic conditions and related subaerial exposure of the Pilkarar sediments. The obtained $\delta^{13}C$ values are suggestive of paleovegetation cover mixed C3 and C4 type plants with dominance of C3 plants (Salomons and Mook, 1986a,b; Quade et al., 1989; Purvis and Wright, 1991; Wright et al., 1993; Tanner, 2010). The obtained paleotemperatures of 21.44° C of calcretes from Pilikarar Formation is an indicator of C3 dominated vegetation. According to Yamori et al., (2013), optimum temperature for photosynthesis of C3 plants is around 25°C and that for C4 plants is about 35°C, and their photosynthesis is inhibited at temperatures of about 45° C and 48° C respectively. Thus, paleotemperature estimate of rhizolith from Pilikarar Formation indicate C3-C4 mixed vegetation with dominance of C3 plants. The obtained value of pCO_2(241.5 ppmV) in general indicates semiarid climate at the time of formation of the calcrete (Li et al., 2013).

CONCLUSION

The Pilikarar Formation represent the deposits of alluvial fan on the basis of :

1. Development of bouldery conglomerate lithofacies representing debris flow deposits. The clast composition of these suggests derivation from Vindhyan Supergroup sediments, Deccan trap basalts and laterite.

2. The occurrence of Pilikarar fan at the base of Vindhyan range and its nearness to Son-Narmada North Fault suggest that both tectonics as well as climate played role in generation of debris flows to build the Pilikarar alluvial fan.

3. For the construction of Pilikarar alluvial fan, catastrophic but infrequent primary process of debris flow is responsible while the associated caliche nodules and rhizolith are the result of secondary process operative during inactive period of fan aggradations. The presence of caliche nodules and rhizoliths

particularly in middle part of Pilikarar Formation are suggestive of semi arid climatic conditions and related subaerial exposure, while presence of ferruginous cement in the uppermost part of Pilikarar Formation is suggestive of oxidizing diagenetic conditions undergone by these sediments.

4. The quartzose arenitic nature of these sediments, together with moderately high ZTR index with rounded nature of ultrastable grains along with presence of augite, staurolite, garnet, sillimanite, kyanite, sphene, zoisite, spinel, chlorite, hornblende, anataze; presence of illite, kaolinite and montmorillonite clays; major, trace and rare earth element compositions; suggests mineralogical maturity and recycled nature of Pilikarar sediments derived from mixed provenance of Precambrian granite, metapelite-shale; Vindhyan Supergroup; Deccan trap basalt and laterite.

5. The stable isotopic composition of calcrete of Pilikarar Formation and value of pCO_2 are suggestive meteoric vadose digenesis under moderate paleotemperature related with subaerial exposure of sediments, with dominance C3 type of paleovegetation and then prevailing semiarid conditions.

Acknowledgements:

The first author is thankful to Department of Science and Technology (DST), New Delhi; for financial assistance (SR/S4/ES-477/2009). The authors thank Head, Department of Geology, Savitribai Phule Pune University; for providing necessary facilities during this work. We thank Drs. Abhay Mudholkar, J. N Pattan, G. Parthiban, from NIO, Goa; for providing major oxide and trace, REE data respectively. Dr. D. J. Patil, NGRI, Hyderabad, is thanked for providing C and O stable isotope data.

References

Ali, S., Stattegger, K. D., Garbe-Schönberg, M., Frank, M. , Kraft, S. and Kuhnt, W. (2014). The provenance of Cretaceous to Quaternary sediments in the Tarfaya basin, SW Morocco: Evidence from trace element geochemistry and radiogenic Nd–Sr isotopes. *Journal of African Earth Science*, 90, 64–76.

Armstrong-Altrin, J. S., Lee, Y. I., Kasper-Zubillaga, J. J., and Trejo-Ramírez, E. (2017). Mineralogy and geochemistry of sands along the Manzanillo and El Carrizal beach areas, southern Mexico: implications for palaeoweathering, provenance and tectonic setting. *Geological Journal*, 52, 559-582.

Armstrong-Altrin, J. S., Nagarajan, R., Madhavaraju, J., Rosalez-Hoz, L., Lee, Y. I., Balaram, V., Cruz-Martinez, A., and Avila-Ramirez, G. (2013). Geochemistry of the Jurassic and upper Cretaceous shales from

the Molango Region, Hidalgo, Eastern Mexico: implications of source area weathering, provenance, and tectonic setting. *Comptes Rendus Geosciences*, 345, 185–202.

Bahlburg, H. and Dobrzinski, A. (2009). A review of the Chemical Index of Alteration (*CIA*) and its application to the study of Neoproterozoic glacial deposits and climate transitions, In: Arnaud, E., Halverson, G.P. & Shields, G.A., (Eds.), *The Geological Record of Neoproterozoic Glaciations*. *Geological Society, London, Memoir*, 81 -93.

Banerjee, A. and Banerjee, D. M. (2010). Modal analysis and geochemistry of two sandstones of the Bhander Group (Late Neoproterozoic) in parts of the Central Indian Vindhyan basin and their bearing on the provenance and tectonics.*Journal of Earth System Sciences*, 119,825–839.

Blair, T. C. and McPherson, J. G. (1993). The Trollheim alluvial fan and facies modelrevisited; *Geological Society of America Bulletin*, 105, 564-567.

Blair, T. C. and McPherson, J. G. (1994). Alluvial fans and their natural distinction from rivers based on morphology, hydraulic processes, sedimentary processes and facies assemblages, *Journal of Sedimentary Petrology*, A64, 450-489.

Blair, T. C. and McPherson, J. G. (2009). Processes and forms of alluvial fans. In: Parsons A. J. and Abrahams A.D. (Eds.) *Geomorphology of Desert Environments*, 2nd ed., 413-467.

Blatt, H. (1992).*Sedimentary Petrology*. W. H. Freman and Co. Ltd., NewYork Oxford, IInd Edition, 514p.

Braithwaite, C. J. R. (1989). Displacive calcite and grain breakage in sandstone, *Journal Sedimentary Petrology*, 59, 258-266.

Brlek, M. and Glumec, B. (2014). Stable isotopic signatures of biogenic calcrete marking discontinuity surfaces: a case study from Upper Cretaceous carbonates of central Dalmatia and eastern Istria, Croatia. *Facies*, 60, 773-788.

Brooke, S., Whittaker, A., Watkins, S., and Armitage, J. (2017). Decoding sediment transport dynamics on alluvial fans from spatial changes in grain size, Death Valley, California. GU General Assembly Conference AbstractsVolume 19, 6677.

Buczynski, C. and Chafetz, H. S. (1987). Siliciclastic grain breakage and displacement due to carbonate crystal growth: an example from Lueders Fonnation of North Central Texas, USA. *Sedimentology*, 34, 837-843.

Bull, W. B. (1977). The alluvial fan environment. *Progress in Physical Geography*, 1, 222-270.

Carver, R. E. (Ed.) (1971). Procedures in Sedimentary Petrology. John-Wiley and Sons, New York, 653 p.

Cerling, T. E. (1984). The stable isotopic composition of modern soil carbonate and its relationship to climate.*Earth and Planetary Science Letter*, 71, 229-240.

Cerling, T. E. (1999). Stable carbon isotopes in palaeosol carbonates. In: M. Thiry and R. Simon-Coinçon (Eds.) *Palaeoweathering, Palaeosurfaces and Related Continental Deposits. Special Publication International Association of Sedimentologists* No. 27, 43–60.

Chamyal, L. S., Khadkikar A. S., Malik J. N. and Maurya D. M. (1997). Sedimentology of the Narmada alluvial fan, western India. *Sedimentary Geology*, 107, 263–279.

Chen, L., Steel, R. J., Guo, F., Olariu, C., and Gong, C. (2017). Alluvial fan facies of the

Yongchong Basin: Implications for tectonic and paleoclimatic changes during Late

Cretaceous in SE China, *Journal of Asian Earth Science*, 134, 37-54.

Choubey, V. D. (1971). Narmada Son lineament, India. *Nature Physical Science*, 55, 392-397.

Costa, J. E. (1988). Rheologic, geomorphic, and sedimentologic differentiation of water floods, hyperconcentrated flows, and debris flows. Flood Geomorphology. John Wiley & Sons New York,113-122.

Cox, R., Lowe, D. R. and Cullers, R. L. (1995). The influence of sediment recycling and basement composition on evolution of mudrock chemistry in the southwestern United States. *Geochemica et Cosmochemica Acta*, 59,2919–2940.

Cullers, R. L. (1988). Mineralogical and chemical changes of soil and stream sediment formed by intense weathering of the Danberg granite, Georgia, USA. *Lithos*, 21, 301–314.

Cullers, R. L. (1994). The controls on the major and trace element variation of shales,

siltstones, and sandstones of Pennsylvanian-Permian age from uplifted continental

blocks in Colorado to platform sediment in Kansas, USA. *Geochemica et Cosmochemica Acta*, 58, 4955–4972.

Cullers, R. L. (2000). The geochemistry of shales, siltstones and sandstones of Pennsylvanian-

Permian age, Colorado, USA: implications for provenance and metamorphic studies. *Lithos*, 51, 181–203.

Cullers R. L. and Podkovyrov V. N. (2000). Geochemistry of the Mesoproterozoic Lakhanda

shales in southeastern Yakutia, Russia: implications for mineralogical and provenance control, and recycling. *Precambrian Research*, 104, 77–93.

De Haas, T., Densmore, A. L., Stoffel, M., Suwa, H., Imaizumi, F., Ballesteros-Cánovas, J. A. and Wasklewicz, T., (2018). Avulsions and the spatio-temporal evolution of debris-flow fans. *Earth Science Reviews*, 177, 53-75.

Ekart, D. D., Cerling, T. E., Montañez, I. P. and Tabor, N. J. (1999). A 400 million year carbon isotope record of pedogenic carbonate: implications for paleoatmospheric carbon dioxide. *American Journal of Science*, 299, 805–827.

Fedo, C. M., Nesbitt, H. W. and Young, G. M. (1995). Unravelling the effects of potassium metasomatism in sedimentary rocks and paleosols, with implications for weatheringconditions and provenance. *Geology*, 23, 921-924.

Franke, D., Jens, H. and Matthias, H. (2015). A combined study of radar facies, lithofacies and three-dimensional architecture of an alpine alluvial fan(Illgraben fan, Switzerland). *Sedimentology*, 62, 57–86.

Friedman, I. and O'Neil, J. R. (1977). Compilation of stable isotope fractionation factors of geochemical interest. In: Fleischer M. (Ed.) *Data of Geochemistry*.*U.S.Geological Survey Professional Paper* 440 KK, pp. 1-12.

Galehouse, J. S. (1971). Sedimentation analysis, In: Carver R. E. (Ed.) *Procedures in Sedimentary Petrology*, John Wiley & Sons, New York, pp. 69-94.

Garzanti, E., Padoan, M., Andò, S., Resentini, A., Vezzoli, G., and Lustrino, M., (2013a). Weathering and relative durability of detrital minerals in equatorial climate: Sand petrology and geochemistry in the East African Rift. *Journal of Geology*, 121, 547–580.

Garzanti, E., Padoan, M., Peruta, L., Setti, M., Najman, Y., and Villa, I. M., (2013b). Weathering geochemistry and Sr-Nd fingerprints of equatorial upper Nile and Congo muds. *Geochemistry Geophysics Geosystems*,14, 292–316.

Ghinassi, M. and Ielpi, A.(2016).Morphodynamics and facies architecture of stream flow-dominated, sand-rich alluvial fans, Pleistocene Upper Valdarno Basin, Italy.*Geological Society of London Special Publications*,440, https://doi.org/10.1144/SP440.1

Geological Survey of India (1993). Geological map of Son-Narmada-Tapti Lineament Zone, Central India, Special Project CRUMANSONATA, 1881-89, *Unpublished Report Geological Survey of India.*

Ghosh, D. B. (1976). The nature of Narmada Son Lineament. *Miscellaneous Publication Geological Survey of India*, 34, 119-133.

Gupta, H., Chakrapani, G. J., Selvaraj, K. and Kao, S. J. (2011). The fluvial geochemistry, contributions of silicate, carbonate and saline-alkaline components to chemical weathering flux and controlling parameters: Narmada River (Deccan Traps), India, *Geochemica et Cosmochemica Acta*, 75, 800-824.

Harnois, L. (1988). The CIW index: A new chemical index of weathering. *Sedimentary Geology*, 55**,** 319–322.

Hays, P. D. and Grossman, E. L. (1991). Oxygen isotope in meteoric calcite cements as indicators of continental paleoclimate. *Geology*, 19, 441-444.

Henderson, P. (1984).*Rare Earth Element Geochemistry*, Elsevier, Amsterdam, 510 p.

Herron, M. M. (1988). Geochemical classifications of terrigeneous sands and shales from core to log data. *Journal of Sedimentary Petrology*, 58, 820-829.

Hubert, J. F. (1962). A zircon-tourmaline-rutile maturity index and the interdependence of the composition of heavy mineral assemblage with gross composition and the texture of sandstones. *Journal of Sedimentary Petrology*, 32, 440-450.

Ingram R. L. (1971). Sieve analysis, In: Carver R. E. (Ed.) *Procedures in Sedimentary Petrology*, John Wiley and Sons, New York, pp. 49-68.

Iverson, R. M. (1997). The physics of debris flows. *Reviews of Geophysics*, 35, 245-296.

Jakob, N. and Hungr, O. (2005). *Debris flow hazards and related phenomena*. Springer Praxix Books, Chichester, UK. 739p.

Jafarzadeh, M. and Hosseini-Barzi, M. (2008). Petrography and geochemistry of Ahwaz Sandstone Member of Asmari Formation, Zagros, Iran: implications on provenance and tectonic setting. *Revista Mexicana de Ciencias Geológicas*, 25, 247-260.

Johnson, A. M. (1970). Formation of debris flow deposits.In: *Physical Processes inGeology*, San Francisco, Freeman, Cooper, 433-448.

Kale, V. S. (1986). The Narmada- Son structure A (Precambrian) reappraisal. Proceedings of Seminar 'Crustal Dynamics', Indian Geophysical Union, Hyderabad, 140-160.

Kamber, B. S., Greig, A., and Collerson, K. D. (2005). A new estimate for the composition of weathered young upper continental crust from alluvial sediments, Queensland, Australia. *Geochimica et Cosmochimica Acta* 69, 1041-1058.

Kettanah, Y. A., Kettanah, M. Y. and Wach, G. D. (2014). Provenance, diagenesis and reservoir quality of the Upper Triassic Wolfiville Formation, Bay of Fundy, Nova Scotia, Canada. *In:* Scott R. A., Smyth H. R., Morton A. C. and Richardson N. (Eds.) *Sediment Provenance studies in Hydrocarbon exploration and Production, Geological Society of London Special Publication*., 386,75-110.

Khadkikar, A. S., Chamyal, L. S. and Ramesh, R. (2000). The character and genesis of calcretes in semi-arid to sub-humid alluvial systems and its bearing on the interpretation of ancient climates. *Palaeogeography Palaeoclimatology Palaeoecology*, 142, 239–262.

Li, X., Jenkyns, H. C, Zhang, C., Wang, Y., Liu, L. and Cao, K. (2013).Carbon isotope signatures of pedogenic carbonates from SE China: rapid atmospheric pCO2 changes during middle–late EarlyCretaceous time. *Geological Magazine*,151, 1-20Cambridge university press.

Liu, S., Lin, G., Liu, Y., Zhou, Y., Gong, F. and Yan, Y. (2007).Geochemistry of Middle Oligocene–Pliocene sandstones from the Nanpu Sag, Bohai Bay Basin (Eastern China):Implications for provenance, weathering, and tectonic setting, *Geochemical Journal*, 41, 359-378.

Lodders, K., and Fegley, B. (1998). The planetary scientist's companion. Oxford University Press, New York, Oxford, 371p.

Longman, M. W. (1980). Carbonate diagenetic texture from near surface diagenetic environments, *Bulletin American Association of Petroleum Geologists*,64, 461-487.

Mahoney, J. J. (1988). Deccan Traps, In: Macdougall J. D. (Ed.), *Continental Flood Basalts*, Springer, Dordrecht, 151-194.

Mason, B. and Moore, C. B. (1982). *Principles of Geochemistry*, John Wiley and sons, New York, 344 p.

McLennan, S. M. (1989). Rare earth elements in Sedimentary rocks: Influence of Provenance and Sedimentary Processes. *Reviews in Mineralogy*,21, 169-200.

McLennan, S. M. and Taylor, S. R. (1991). Sedimentary rocks and crustal evolution revisited: tectonic setting and secular trends. *Journal of Geology*, 99, 1-21.

McLennan, S. M., Hemming, S., McDaniel, D. K. and Hanson, G. N. (1993). Geochemical approaches to sedimentation, provenance and tectonics. *Special papers Geological Society of America*, 21-21.

Miall, A. D. (2006).*The Geology of Fluvial Deposits Sedimentary Facies, Basin*

Analysis, and Petroleum Geology. Springer-Verlag Berlin Hedelberg, 582 p.

Mishra, D. C. (2015). Plume and Plate tectonics model for formation of some Proterozoic basins of India, along contemporary mobile belts: Mahakoshal-Bijawar, Vindhyan and Cuddapah basins. *Journal of The Geological Society of India*, 85, 525-536.

Mohammadi, N., Rais, S. and Habib, T. (2014).Provenance, tectonic setting and paleoclimate of Upper Bhander Sandstone in parts of Raisen district of Madhya Pradesh (India). *International Journal of Advance Earth and Environment Science*, 2, 39-45.

Morse, J. W. and Mackenzie, F. T. (1990). Geochemistry of Sedimentary Carbonates, Elsevier Amsterdam, New York, Developments in Sedimentology, 48,707 p.

Morton, A. C. and Hallsworth, C.R. (1994). Identifying provenance-specific features of detrital heavy mineral assemblages in sandstones. *Sedimentary Geology*, 90, 241-256.

Morton, A. C. and Hallsworth, C. R. (1999). Processes controlling the composition of heavy mineral assemblages in sandstones. *Sedimentary Geology*, 124, 3-29.

Morton, A.and Milne, A. (2012). Heavy mineral stratigraphic analysis on the Clair Field, UK, west of Shetlands: a unique real-time solution for red-bed correlation while drilling. *Petroleum Geoscience*, 18, 115 –128.

Nesbitt, H. W. and Young, G. M. (1982). Early Proterozoic climates and plate motions inferred from major element chemistry of lutites. *Nature*, 299, 715–717.

Nesbitt, H. W. and Young, G. M. (1984). Prediction of some weathering trends of plutonic and volcanic rocks based on thermodynamic and kinetic considerations. *Geochemica et Cosmochemica Acta*, 48, 1523-1534.

Nesbitt, H. W. and Young, G. M. (1989). Formation and diagenesis of weathering profiles. *Journal of Geology*, 97, 129–147.

Ohta, T. and Arai, H. (2007).Statistical empirical index of chemical weathering in igneous

rocks: A new tool for evaluating the degree of weathering. *Chemical Geology*, 240, 280-297.

Okada, H. (1971). Classification of sandstone: Analysis and proposal. *Journal of Geology*, 79, 509-525.

Parker, A. (1970). An index of weathering for silicate rocks. *Geological Magazine*, 107, 501-504.

Pettijohn, F. J., Potter, P. E and Siever, R. (1972). *Sand and Sandstones*, Springer Verlag New York.

Piper, D. Z. and Bau, M. (2013). Normalized Rare Earth Elements in Water, Sediments, and Wine: Identifying Sources and Environmental Redox Conditions. *American Journal of Analytical Chemistry*, 4, 69-83.

Purevjav, N. and Roser, B. (2013). Geochemistry of Silurian–Carboniferous sedimentary rocks of the Ulaanbaatarterrane, Hangay–Hentey belt, central Mongolia: Provenance, paleoweathering, tectonic setting, and relationship with the neighbouring Tsetserleg terrane. *Chemie der Erde*, 73, 481– 493.

Purvis, K. and Wright, V. P. (1991).Calcretes related to phreatophytic vegetation from

Middle Triassic Otter Sandstone of South west England. *Sedimentology*, 38, 539-551.

Quade, J., Cerling, T. E. and Bowman, J.R. (1989). Development of monsoon revealed by marked ecological shift during the latest Miocene in the Northern Pakistan, *Nature*, 342, 163-166.

Reading, H. Q.(1981).*Sedimentary Environments and Facies*, Blackwell Scientific Publications, Oxford, London, 569 p.

Reading, H. Q. (2006).*Sedimentary Environments: Processes, Facies, and Stratigraphy*, Blackwell Publishing, India, 688p.

Reineck, H. E. and Singh, I. B. (1980). *Depositional Sedimentary environments*, Springer Verlag, Berlin, Heidelburg, New York, 549 p.

Renwick, W. H. (1977).Erosion caused by intense rainfall in a small catchment in New York State, *Geology*, 5, 361-364.

Robinson, S. A., Andrews, J. E., Hesselbo, S. P., Radley, J. D., Dennis, P. F., Harding, I. C., and Allen, P. (2002). Atmospheric pCO2 and depositional environment from stable-isotope geochemistry of calcrete nodules (Barremian, Lower Cretaceous, Wealden Beds, England). *Journal of Geological Society of London*, 159, 215-224.

Rollinson, H. (1993). *Using geochemical data: evaluation, presentation, interpretation*. Pearson Education Ltd, Essex, London. 352 .

Roser, B. P. and Korsch, R. J. (1986). Determination of tectonic setting of sandstone–mudstone suites using SiO_2 content and K_2O/Na_2O ratio. *Journal of Geology*, 94, 635–650.

Roser, B. P and Korsch, R. J. (1988). Provenance signatures of sandstone-mudstone suites determined using discriminant function analysis of major of major element data. *Chemical Geology*, 67, 119-139.

Roser, B. P., Cooper, R. A., Nathan, S. and Tulloch, A. J. (1996). Reconnaissance sandstone geochemistry, provenance and tectonic setting of the lower Paleozoic terrains of the west coast and Nelson, New Zeland. *New Zeland Journal of Geology and Geophysics*, 39, 1-16.

Rudnick, R. L. and Gao, S. (2003).Composition of the continental crust In: Rudnick, R.L,

Holland, H.D and Turekian, K. K. (Eds) *Treatise on Geochemistry*, 3,1-64.

Salomons, W. and Mook, W. G. (1986 a). Isotope geochemistry of carbonate dissolution and reprecipitation in soils. *Soil Science*, 122, 15-24.

Salmons, W. and Mook, W. G. (1986b). Isotope geochemistry of carbonates in weathering zone, In: Fritz P. and Frontes J. Ch. (Eds.) *Handbook of Environmental Isotope Geochemistry*. New York,2, 239-269.

Seth, H., Ray, J. S., Ray, R., Vanderkluysen, L., Mahoney, J. J., Kumar, A., Shukla, A. D., Das, P., Adhikari, S. and Jana, B. (2009). Geology and geochemistry of Pachmarhi dykes and sills, Satpura Gondwana basin, Central India: Problems of dikes-sill-flow correlation in the Deccan Traps. *Contribution to Mineralogy and Petrology*, 158, 357-380.

Sohn, Y. K., Rhee, C. V. and Kim, B. C. (1999). Debris flow and hyperconcentrated flood-flow deposits in an Alluvial fan, Northwestern part of the Cretaceous Yongdong basin, Central Korea. Journal of Geology, 107, 111-132.

Soni, M. K., Chakraborty, S. and Jain, V. K. (1987).Vindhyan Supergroup- A review, In: *Purana Basins of Peninsular India (Middle to Late Proterozoic), GeologicalSociety of India Memoir No*. 6, 87-138.

Srivastava, P. (2001). Paleoclimatic implications of pedogenic carbonates in Holocene soils of Gangatic plains, India. *Palaeogeography Palaeoclimatology Palaeoecology*, 172, 207-222.

Stainstreet, I. G. and McCarthy, T. S.(1993). The Okavango fan and the classification of subaerial fan systems, *Sedimentary Geology*, 85, 115-133.

Talma, A. S. and Netterberg, F. (1983).Stable isotope abundances in calcretes. *Geological Society of London Special Publication*, 11, 221-233.

Tandon, S. K. and Friend, P. F. (1989). Near surface shrinkage and carbonate replacement processes Arran Cornstone Formation, Scotland. *Sedimentology*, 36, 1113-1126.

Tanner, L. H. (2010). Continental carbonates as indicators of paleoclimate. In: Alonso-Zarza A.M. , Tanner L. H. (Eds.) *Carbonates in continental settings: geochemistry, diagenesis and applications. Developments in Sedimentology*, 62, 179-206.

Tao, H., Sun, S., Wang, Q., Yang, X., and Jiang, L. (2014). Petrography and geochemistry of Lower Carboniferous greywacke and mudstones in Northeast Junggar, China: Implications for provenance, source weathering, and tectonic setting. *Journal of Asian Earth Sciences*, 87, 11-25.

Tawfik, H. A., Salah, M. K., Maejima, W., Armstrong-Altrin, J. S., Abdel-Hameed, A. M. T., and El Ghandour, M. M. (2017). Petrography and geochemistry of the Lower Miocene Moghra sandstones, Qattara Depression, north Western Desert, Egypt. *Geological Journal*, pp. 1-16.DOI: 10.1002/gj.3025.

Tiwari, M. P. and Bhai, H.Y. (1997). Quaternary stratigraphy of the Narmada Valley. *Geological Survey of India Special Publication* No.46, 33-63.

Tucker, M. E. (2001). *Sedimentary Petrology*, 3rded., Blackwell Science, Oxford UK, 262 p.

Tucker, M. E. and Wright, V. P. (1990). *Carbonate Sedimentology*, Blackwell Scientific Publications, Oxford London, 482 p.

Vaidyanathan, R. and Ramakrishnan, M. (2008). *Geology of India*. Geological Society of India, 2, 833-906.

Verma, S. P. and Armstrong-Altrin, J. S. (2013). New multi-dimensional diagrams for

tectonic discrimination of siliciclastic sediments and their application to Precambrian basins. *Chemical Geology*, 355, 117-133.

Verma, S. P., and Armstrong-Altrin, J. S. (2016). Geochemical discrimination of siliciclastic

sediments from active and passive margin settings. *Sedimentary Geology*, 332, 1-12.

Verma, R. K. and Banarjee, P. (1992). Nature of continental crust along the Narmada–Son Lineament, inferred from gravity and deep seismic sounding data. *Tectonophysics*, 202, 375–397.

Visher, G. S. (1969). Grain size distribution and depositional processes. *Journal of Sedimentary Petrology*, 49, 41-62.

Weaver, C. E. (1989). *Clays, Muds and Shales*. Elsevier Science Publishing Company Inc., NewYork, 819 p.

Wright, V. P., Turner, M. S., Andrews, J. E. and Spiro, B. (1993). Morphology and significance of supermature calcretes from the Upper Old Red Sandstone of Scotland. *Journal of Geological Society of London*, 150, 871-883.

Xie, Y., Yuan, F., Zhan, T., Kang, C. and Chi, Y. (2017). Geochemical and isotopic characteristics of sediments for the Hulun Buir Sandy Land, northeast China: implication for weathering, recycling and dust provenance. *Catena*, 160, 170-184.

Young, W. S. (1976). Petrographic textures of detrital polycrystalline quartz as an aid to interpret crystalline source rock. *Journal of Sedimentary Petrology*, 46, 595-603.